CD146 is a coreceptor for VEGFR-2 in tumor angiogenesis

Tianxia Jiang,[1] Jie Zhuang,[1] Hongxia Duan,[1] Yongting Luo,[1] Qiqun Zeng,[1] Kelong Fan,[1] Huiwen Yan,[1] Di Lu,[1] Zhongde Ye,[1] Junfeng Hao,[1] Jing Feng,[1] Dongling Yang,[1] and Xiyun Yan[1]

[1]Key Laboratory of Protein and Peptide Pharmaceutical, National Laboratory of Biomacromolecules, Chinese Academy of Sciences–University of Tokyo Joint Laboratory of Structural Virology and Immunology, Institute of Biophysics, Chinese Academy of Sciences, Beijing, China

CD146 is a novel endothelial biomarker and plays an essential role in angiogenesis; however, its role in the molecular mechanism underlying angiogenesis remains poorly understood. In the present study, we show that CD146 interacts directly with VEGFR-2 on endothelial cells and at the molecular level and identify the structural basis of CD146 binding to VEGFR-2. In addition, we show that CD146 is required in VEGF-induced VEGFR-2 phosphorylation, AKT/p38 MAPKs/NF-κB activation, and thus promotion of endothelial cell migration and microvascular formation. Furthermore, we show that anti-CD146 AA98 or CD146 siRNA abrogates all VEGFR-2 activation induced by VEGF. An in vivo angiogenesis assay showed that VEGF-promoted microvascular formation was impaired in the endothelial conditional knockout of CD146 ($CD146^{EC\text{-}KO}$). Our animal experiments demonstrated that anti-CD146 (AA98) and anti-VEGF (bevacizumab) have an additive inhibitory effect on xenografted human pancreatic and melanoma tumors. The results of the present study suggest that CD146 is a new coreceptor for VEGFR-2 and is therefore a promising target for blocking tumor-related angiogenesis. (*Blood*. 2012;120(11):2330-2339)

Introduction

Angiogenesis, the formation of new capillaries from preexisting microvasculature, is a complex and crucial process during embryogenesis, the female reproductive cycle, chronic inflammatory disorders, and tumor growth.[1] Many tumor masses secrete several kinds of angiogenic factors, such as VEGF, TGFα, and TNF, to promote blood vessel formation that eventually functions as a route for tumor metastasis.[2]

Among these angiogenic factors, VEGF is the most prominent one and belongs to a family that includes VEGF-A, VEGF-B, VEGF-C, VEGF-D, VEGF-E, and placental growth factor. VEGFs bind to 3 associated transmembrane tyrosine kinase receptors known as VEGFR-1(Flt-1), VEGFR-2 (KDR or Flk-1), and VEGFR-3(Flt-3). VEGFR-2 is a key receptor for the development of the blood vasculature[3] and VEGFR-3 is mainly involved in lymphogenesis.[4] Therefore, targeting the VEGF-A/VEGFR-2 pathway has become an attractive strategy for antiangiogenesis and tumor therapy.[2,5] For example, bevacizumab, a very popular anti–VEGF-A Ab, has been used for the treatment of several cancers.[6-9] However, it was reported recently that some patients are intrinsically refractory to or have acquired resistance to bevacizumab.[10] Therefore, the development of new or adjunct therapies would be of great benefit to patients.

CD146 is a cell-adhesion molecule belonging to the immunoglobulin superfamily. It was originally considered as a melanoma marker promoting melanoma growth and metastasis.[11] Recently, increasing evidence suggests that CD146 is an endothelial biomarker that promotes angiogenesis.[12,13] CD146 knockdown was shown to impair cardiovascular development and to block tumor angiogenesis in zebrafish.[14] Our previous work showed that an anti-CD146 Ab, AA98, inhibited endothelial cell migration and angiogenesis and human tumor growth in xenografted mice.[15] In addition, we found that CD146 plays an important role in cell migration that is specifically detected in invasive but not in noninvasive intermediate trophoblasts and in preeclampsia.[16,17] Recently, we reported that CD146 is an epithelial-mesenchymal transition inducer and promotes the invasion of triple-negative breast cancer.[18]

Although CD146 has been considered as a receptor in endothelial cells, its ligand is still unknown.[19] Our previous studies showed that tumor secretion induced CD146 dimerization, p38 MAPKs/NF-κB activation, and the up-regulation of many angiogenic genes, including VEGF, MMP-9, and IL-8, and that anti-CD146 mAb (AA98) interfered with this CD146-mediated signaling.[20,21] In addition, Anfosso et al found that CD146 associated with tyrosine kinase $p59^{Fyn}$ to phosphorylate $p125^{Fak}$ and paxillin, thus promoting endothelial cell migration.[22,23] However, the molecular mechanism of how CD146 functions as a receptor in angiogenesis remains poorly understood.

In the present study, we show for the first time that CD146 interacts with VEGFR-2 in the endothelium and subsequently promotes angiogenesis in vitro and in vivo. Moreover, this CD146 and VEGFR-2 interaction and its mediated signal transduction could be blocked by anti-CD146 mAb AA98 or CD146 siRNA. Most importantly, our animal experiments demonstrated that combination therapy with anti-CD146 AA98 and anti-VEGF (bevacizumab) has an additive killing effect on both human pancreatic carcinoma and human melanoma. Our findings not only reveal the mechanism of how CD146 plays an important role in angiogenesis, but also provide a novel insight for combinatorial therapy of tumor angiogenesis.

Submitted January 22, 2012; accepted June 17, 2012. Prepublished online as *Blood* First Edition paper, June 20, 2012; DOI 10.1182/blood-2012-01-406108.

There is an Inside *Blood* commentary on this article in this issue.

The online version of this article contains a data supplement.

The publication costs of this article were defrayed in part by page charge payment. Therefore, and solely to indicate this fact, this article is hereby marked "advertisement" in accordance with 18 USC section 1734.

Methods

Cells and animals

Human pancreatic carcinoma SW1990 cells and the human melanoma A375 cells were obtained from the ATCC. Human umbilical vein endothelial cells (HUVECs) were from CellSystems Biotechnologie Vertrieb. For the generation of CD146-expressing stable human embryonic kidney cell line HEK293T clones, HEK293T cells were transfected with human PBudCE4.1-CD146 using the Fugene HD method (Roche) and selected using zeocin (500 μg/mL). HEK293T cells stably transfected with CD146 were cultured in DMEM (Gibco Life Technologies) with 1 g/L of glucose, 10% FCS, 100 U/mL of penicillin, and 100 μg/mL of streptomycin. All cells were grown at 37°C and 5% CO_2.

All animal experiments were performed in compliance with the guidelines for the care and use of laboratory animals and were approved by the Biomedical Research Ethics Committee of the Institute of Biophysics, Chinese Academy of Sciences (Beijing, China). BALB/c nude mice were obtained from the Animal Center of the Chinese Academy of Medical Science (Beijing, China). $Tek^{cre/+}CD146^{floxed/floxed}$ mice were generated using a Cre/loxP recombination system. $Tek^{+/+}CD146^{floxed/floxed}$ mice were backcrossed to a C57BL/6J background for a minimum of 9 generations for obtaining $Tek^{cre/+}CD146^{floxed/floxed}$ mice ($CD146^{EC\text{-}KO}$). $Tek^{+/+}CD146^{floxed/floxed}$ (wild-type) mice were used as controls in Matrigel plug assays. Genotyping of each generation was carried out using PCR. The complete absence of CD146 from the endothelial cells of vascular vessels was confirmed using immunohistochemistry and immunofluorescence.

Abs and reagents

The mouse anti–human CD146 mAbs AA98[12] and AA1[24] were produced in our laboratory. Bevacizumab was from Roche. Goat anti–rabbit Alexa Fluor 555 and goat anti–rat Alexa Fluor 488 were from Invitrogen. Mouse IgG (mIgG), human IgG (hIgG), and FLAG (clone M2) were from Sigma-Aldrich. Abs against human NF-κB p50 and IκBα were from Santa Cruz Biotechnology. Abs specific for Flk-1, phospho-p38 MAPK, p38 MAPK, phospho–NF-κB p65 (Ser536), phospho-Erk, p44/42MAPK, and phospho-p44/42 MAPK (T202/Y204) were from Cell Signaling Technology. Abs against phospho–VEGFR-2 (Tyr 1214) and phospho-AKT (Ser 473) were from Signalway Antibody. HRP-conjugated goat anti–mouse or rabbit IgG were from GE Healthcare. Ab specific for CD31 was from Abcam. Rat anti–human CD146 (clone ME-9F1) was from BD Biosciences. Biotin-conjugated secondary Abs and HRP-conjugated streptavidin were from Dianova. DAPI was from Roche.

Human recombinant VEGF-A165 was obtained from Upstate Biotechnology. Goat serum and the DAB substrate system were from Santa Cruz Biotechnology. Enhanced chemiluminescence assay kits were from Pierce. Growth factor–reduced Matrigel was from BD Biosciences.

Constructs and transfection

pCDNA3.1-(b)-CD146, pCDNA3.1-(b)-CD146/C452A, and Flag-CD146-△KKGK have been described previously.[21,25] The moesin construct lacking the actin-binding domain (MSN-△ABD) was generated by a PCR-based approach using Flag-MSN as a template. Fugene HD–mediated transfection was used according to the manufacturer's instructions.

RNA interference

Double-stranded RNAs (dsRNA) targeting CDS 410-428 of CD146 and CDS 1562-1580 of green fluorescent protein (GFP), respectively, were synthesized by Invitrogen using sequences described previously.[21]

For siRNA transfections, HUVECs were transfected with 50nM concentrations of either GFP siRNA or CD146 siRNA using the Fugene HD method. Cells were then incubated for 36 hours at 37°C and 5% CO_2.

In vitro pull-down assays

For in vitro pull-down assays, 0.15 μg of Fc or Fc-sVEGFR-2 was conjugated to protein G agarose beads (Santa Cruz Biotechnology). The beads were then incubated with 0.15 μg of His-sCD146 protein for 1 hour at 4°C. Proteins bound to the beads were then boiled in sample loading buffer and subjected to immunoblotting analysis.

Coimmunoprecipitation

HUVECs were lysed in a culture dish by adding 0.5 mL of ice-cold RIPA lysis buffer for 30 minutes. The supernatants were collected by centrifugation at 12 000*g* for 10 minutes at 4°C and then precleared with protein G-Sepharose to remove the protein G–bound proteins. The cleared lysates were then incubated with Abs at 4°C overnight, followed by incubation with protein G-Sepharose for 4 hours. Immunoprecipitates were washed 3 times with lysis buffer and then boiled for 5 minutes in loading buffer.

Activation of RTKs and downstream signals

Serum-starved HUVECs (24 hours) were incubated with blocking reagents (50 μg/mL of the mAb AA98 or AA1) or transfected with siRNA (CD146-siRNA or GFP-siRNA) before induction with VEGF-A165 (50 ng/mL) at 37°C for 10 minutes, 30 minutes, or 12 hours for analysis of the activation of VEGFR-2, p38/AKT/Erk, and NF-κB, respectively. Cells were washed with ice-cold PBS, lysed in RIPA lysis buffer, and then subjected to Western blotting as described.[25] Blots were probed separately with antiphosphorylated Abs against VEGFR-2, Erk, p38, and AKT, and then stripped (62.5mM Tris, pH 6.8, 2% SDS, 0.8% DTT) and reprobed with their corresponding specific Abs as a loading control.

Immunofluorescence

Cells were plated on slides cultured in 6-well plates and then subjected to the appropriate treatments. After stimulation for 24 hours with VEGF-A165 (50 ng/mL), the cells were washed with PBS, fixed in acetone/methanol (1:1) for 30 seconds, permeabilized with 0.1% Triton X-100, blocked with 5% normal goat serum for 60 minutes at 37°C, and then incubated with anti-p65 or anti-p50 for 1 hour. Coverslips were subsequently examined with a confocal laser scanning microscope (Olympus FLUOVIEW FV 1000) with an Olympus IX81 digital camera using 20×/0.75 numeric aperture objective.

Tube formation

The tube formation assay was performed as described by Nagata et al.[26] Tube formation was observed under an inverted microscope (Eclipse model TS100; Nikon). Images were captured with a CCD color camera (model KP-D20AU; Hitachi) attached to the microscope using 4×/0.13 numeric aperture and tube length was measured using ImageJ Version 1.41o software.

Cell migration assay

Cell migration was assayed using a modified Boyden chamber assay (8-μm pore size; Costar; Corning) as described previously.[27] After the appropriate treatments, cells were trypsinized, washed, and resuspended in fresh serum-free medium (10 000 cells per well). After incubation at 37°C overnight, cells remaining at the upper surface of the membrane were removed using a swab and cells that had migrated to the lower membrane surface, which are representative of migrated cells, were fixed with 4% paraformaldehyde and stained with Giemsa solution. Pictures were taken on a OLYMPUS BX51 microscope with a UPlanFL N digital camera using 4×/0.13 numeric aperture objective. Cells migrating through the filter were counted and plotted as the number of migrating cells per optic field.

Immunohistochemistry

For 3,3′-diaminobenzidine (DAB) staining, paraffin-embedded tissue sections were deparaffinized and stained first with an Ab specific for CD31 and then with biotin-conjugated secondary Abs (1:1000), followed by HRP-conjugated streptavidin (Dianova). The sections were finally counterstained with hematoxylin. The number of blood vessels per tumor in each group was quantified in at least 10 random areas per section. Images were taken on a OLYMPUS BX51 microscope with a UPlanFL N digital camera using 10×/0.3 numeric aperture objective.

For immunohistofluorescence, sections 5 μm in thickness were deparaffinized and stained with Abs specific for CD31 and CD146, followed by

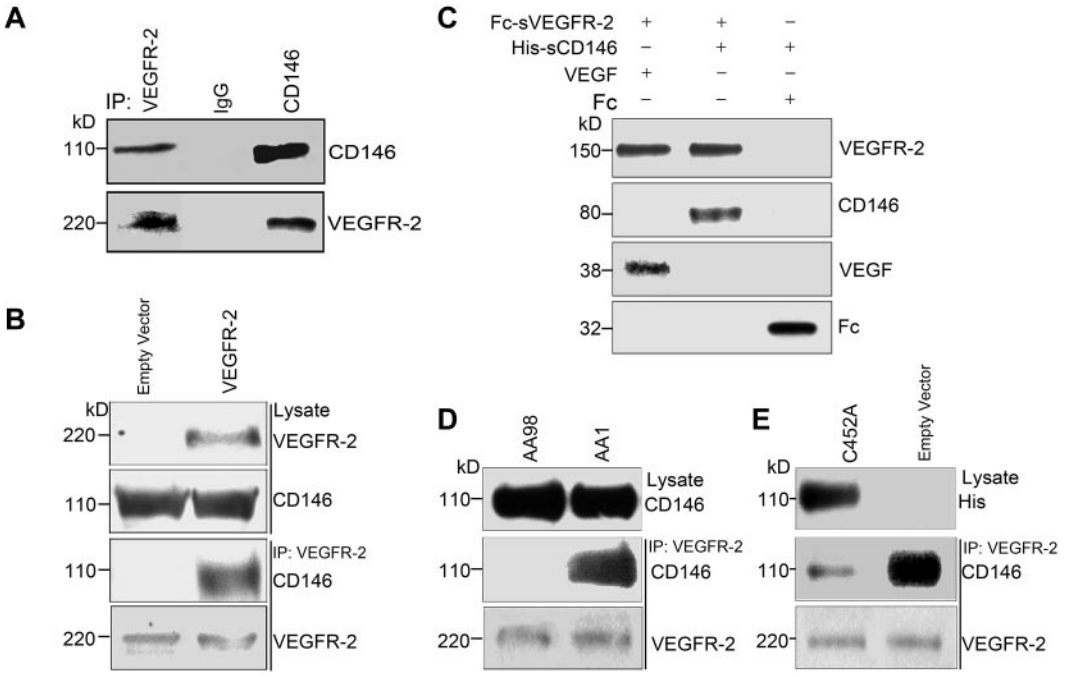

Figure 1. CD146 interacts directly with VEGFR-2. (A) Co-IP assays showed that endogenous CD146 associates with VEGFR-2 in HUVECs. CD146 and VEGFR-2 from cell lysates were immunoprecipitated with anti-CD146 mAb AA1 and anti–VEGFR-2, respectively. Western blotting was performed using anti–VEGFR-2 Ab and mAb AA1. (B) Co-IP assays showed the association of CD146 and VEGFR-2 in CD146-expressing HEK293T cells. Cells were transiently transfected with the VEGFR-2–expressing construct or empty vectors. Proteins were precipitated by anti–VEGFR-2 Ab and examined by immunoblot using Abs against CD146. (C) Direct interaction between the sCD146 and sVEGFR-2 in vitro. Fc-VEGFR2 was first bound to protein G beads, which were then incubated with His-sCD146. Bound proteins were subsequently analyzed by Western blotting. The interaction between VEGF and Fc–VEGFR-2 served as a positive control and Fc served as a negative control. (D) The interaction between CD146 and VEGFR-2 in HUVECs was blocked by anti-CD146 AA98, but not by AA1. HUVECs were first treated with anti-CD146, AA98, or AA1 before immunoprecipitation with VEGFR-2 Ab and Western blotting with CD146 Ab. Cell lysates were blotted with anti-CD146 mAb AA1. (E) Mutant CD146/C452A impaired the interaction between CD146 and VEGFR-2. HUVECs transfected with CD146/C452A or an empty vector were immunoprecipitated with anti–VEGFR-2 and then immunoblotted with anti–VEGFR-2 or AA1. Cell lysates were blotted with anti-his Ab targeting CD146/C452A-His.

fluorescent-labeled secondary Abs. Nuclei were stained with DAPI. Pictures were taken with a confocal laser scanning microscope (Olympus FV 1000) with an Olympus IX81 digital camera using 20×/0.75 numeric aperture objective.

In vivo angiogenesis assay

Age- and sex-matched $CD146^{EC\text{-}KO}$ and wild-type mice were used. Mice were injected with 200 μL of growth factor–reduced Matrigel containing 60 units/mL of heparin (Sigma-Aldrich), mixed with VEGF-A165 (20 ng/mL), and killed 7 days after implantation. The Matrigel plugs were dissected out immediately and blood-vessel infiltration was quantified by analyzing the CD31-stained paraffin sections (as described in "Immunohistochemistry").

Animal experiment

Female 4-week-old BALB/c nude mice were kept under specific pathogen–free conditions. Xenografts of human tumor cell lines were produced by injecting tumor cells (1×10^7 resuspended in PBS) subcutaneously into the backs of the mice. When tumors reached a diameter of 3-5 mm, the mice were grouped (10 mice per group) and administered IP with purified mAb AA98, AA1, human IgG, mIgG, bevacizumab alone, or bevacizumab plus AA98 at a dose of 200 μg per mouse twice per week. Tumor size was measured twice per week and tumor volume was determined according to the following equation: tumor size = $\text{width}^2 \times \text{length} \times (1/2)$.

Statistical analysis

All experiments were done in triplicate. Data are shown as means ± SEM. Statistical differences were determined by unpaired Student *t* tests. The statistical differences of the in vivo Matrigel plug assay were determined by paired Student *t* tests. $P = .05$ was considered stastically significant.

Results

CD146 interacts with VEGFR-2 in endothelial cells

The coexpression of CD146 and VEGFR-2 on endothelial cells and the finding that tumor secretions containing VEGF and FGF induced CD146-mediated p38 MAPKs/NF-κB signaling led us to hypothesize that CD146 may act as a coreceptor for VEGFR-2. To test this, we performed coimmunoprecipitation (co-IP) experiments to detect the interaction of CD146 and VEGFR-2 in 2 cell lines, HUVECs with endogenous CD146 and VEGFR-2 and VEGFR-2–transfected HEK293T cells. As shown in Figure 1A, in HUVECs, VEGFR-2 was immunoprecipitated by anti-CD146 Ab and CD146 was immunoprecipitated by anti–VEGFR-2 Ab. This result was confirmed in VEGFR-2–transfected HEK293T cells, showing that CD146 was coimmunoprecipitated by anti–VEGFR-2 Ab in HEK293T cells coexpressing VEGFR-2 and CD146, but not in the cells expressing CD146 alone (Figure 1B). In addition, we found that CD146 did not interact with VEGFR-1 (supplemental Figure 7, available on the *Blood* Web site; see the Supplemental Materials link at the top of the online article).

To further investigate whether CD146 interacts directly with VEGFR-2, we performed in vitro pull-down assays using soluble CD146 (His-tagged CD146 extracellular domain, His-sCD146) and soluble VEGFR-2 (Fc-tagged VEGFR-2 extracellular domain, Fc-sVEGFR-2). Our results showed that Fc-sVEGFR-2 was bound specifically to His-tagged CD146 as it bound to VEGF. In contrast, neither Fc nor Fc-beads was bound by His-sCD146 (Figure 1C).

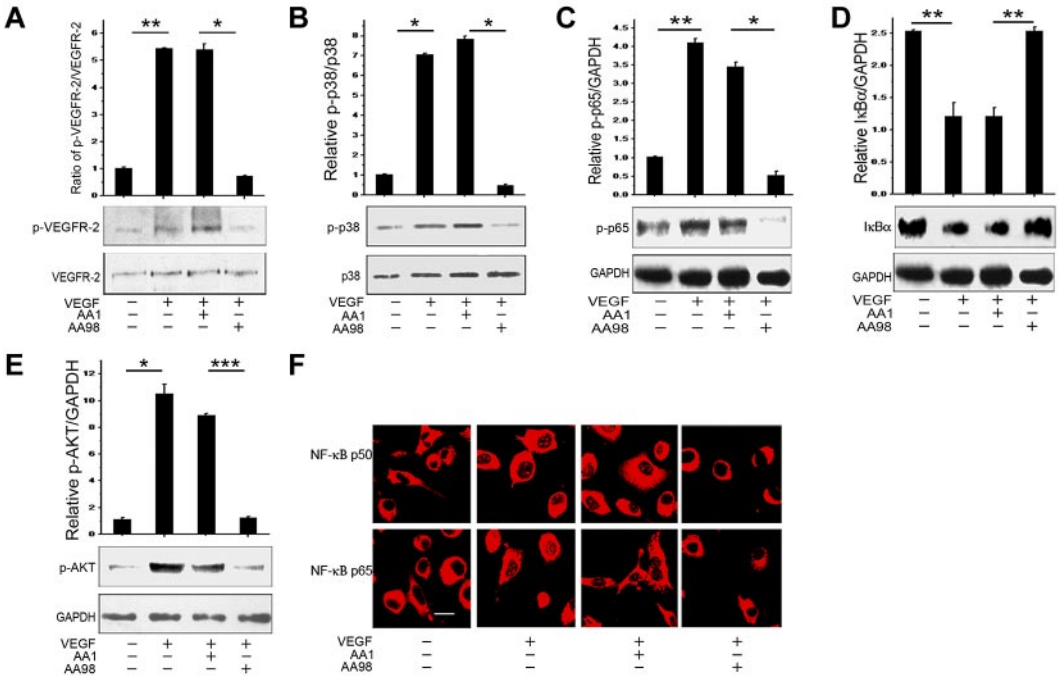

Figure 2. The anti-CD146 mAb AA98 blocks VEGF-induced VEGFR-2 phosphorylation and Akt/p38/NF-κB activation. (A) Phosphorylation of VEGFR-2 induced by VEGF in HUVECs was assessed in the presence of anti-CD146 mAbs AA98 or AA1. Total VEGFR-2 quantification was determined by measuring the band density and then normalizing against internal controls. Results are presented as the means ± SEM of normalized values from 3 independent assays. (B) P38 activation induced by VEGF in the presence of AA98 or AA1. (C-D) NF-κB (p-p65 and IκBα) activation by VEGF in the presence of AA98 or AA1. (E) Akt activation induced by VEGF in the presence of AA98 or AA1. (F) Immunofluorescence showing inhibition of AA98 on the translocation of p65 and p50 from the cytoplasm to nucleus. NF-κB activation was detected using specific anti-p65 (red) and anti-p50 (red) Abs (scale bar indicates 20 μm). *$P < .05$; **$P < .01$.

These data demonstrate a direct interaction between the CD146 extracellular domain and VEGFR-2.

We also investigated whether the interaction of CD146 and VEGFR-2 could be abrogated by anti-CD146 Ab. To test a possible structural basis of CD146 binding to VEGFR-2, we used 2 different anti-CD146 Abs, AA98 and AA1. AA98 recognizes a conformational epitope at C452-C499, whereas AA1 recognizes a linear epitope at amino acids 50-54 in the N-terminal domain.[21] Figure 1D shows that the interaction between CD146 and VEGFR-2 was blocked markedly by AA98 but not by AA1. To confirm this observation, we performed the co-IP experiment in HUVECs using the CD146/C452A mutant and found that the endogenous interaction of CD146 and VEGFR-2 was abrogated by the CD146/C452A mutation (Figure 1E), suggesting that C452 in domain 5 of CD146 contributes to the interaction of CD146 and VEGFR-2. This may explain why the anti-CD146 Ab AA98, but not AA1, inhibited this interaction.

CD146 enhances VEGFR-2 phosphorylation and downstream signaling

Because CD146 associated with VEGFR-2, we next investigated whether CD146 transduces VEGF-activation signals. For this purpose, we used VEGF as a stimulator and anti-CD146 AA98 and CD146 siRNA as inhibitors to evaluate the function of CD146 on the VEGF-induced signaling pathway. As shown in Figure 2, we found that VEGF could induce VEGFR-2 phosphorylation, the p38/IKK/NF-κB signaling cascade, and Akt signal transduction. However, the VEGF-induced downstream signals were abrogated completely by the anti-CD146 mAb AA98 but were not affected by AA1 (Figure 2A-E). Immunofluorescent staining of NF-κB p65 and p50 also confirmed that the nuclear translocation induced by VEGF was suppressed by AA98 treatment, but not by the control Ab, AA1 (Figure 2F). Consistent with these results, HUVECs transfected with a CD146/C452A mutant also inhibited VEGF-activated VEGFR-2 phosphorylation and downstream signal transduction (supplemental Figure 1).

We next analyzed the effect of CD146 siRNA on the activation of signals downstream of VEGFR-2. Our results showed that VEGF-activated VEGFR-2 phosphorylation, the p38/IKK/NF-κB signaling cascade, and Akt signaling were impaired by CD146 knockdown and were rescued after restoring CD146 (Figure 3A-D). In addition, nuclear translocation of NF-κB p65 and p50 induced by VEGF was also inhibited by CD146-siRNA and was reactivated by restoring CD146 expression (Figure 3E). In contrast, VEGF-induced Erk signaling was not affected by either AA98 or CD146-siRNA (supplemental Figure 2), implying that CD146 was mainly involved in the VEGF-induced Akt and p38/IKK/NF-κB pathways.

To determine whether CD146 function is specifically dependent on VEGF, we repeated the experiments with TNFα, another angiogenic factor. We found that neither AA98 nor CD146 siRNA had any effect on the response of NF-κB to TNFα stimulation (supplemental Figure 3), suggesting that the response of CD146 to VEGF is specific.

These data strongly suggest that, as a VEGFR-2 coreceptor, CD146 is involved in regulating VEGF-induced VEGFR-2 downstream signals.

CD146-mediated ERM recruitment is essential for VEGF-mediated signal transduction and cell migration

We reported previously that CD146 interacted physically with Ezrin-Radixin-Moesin (ERM) proteins, leading to the subsequent

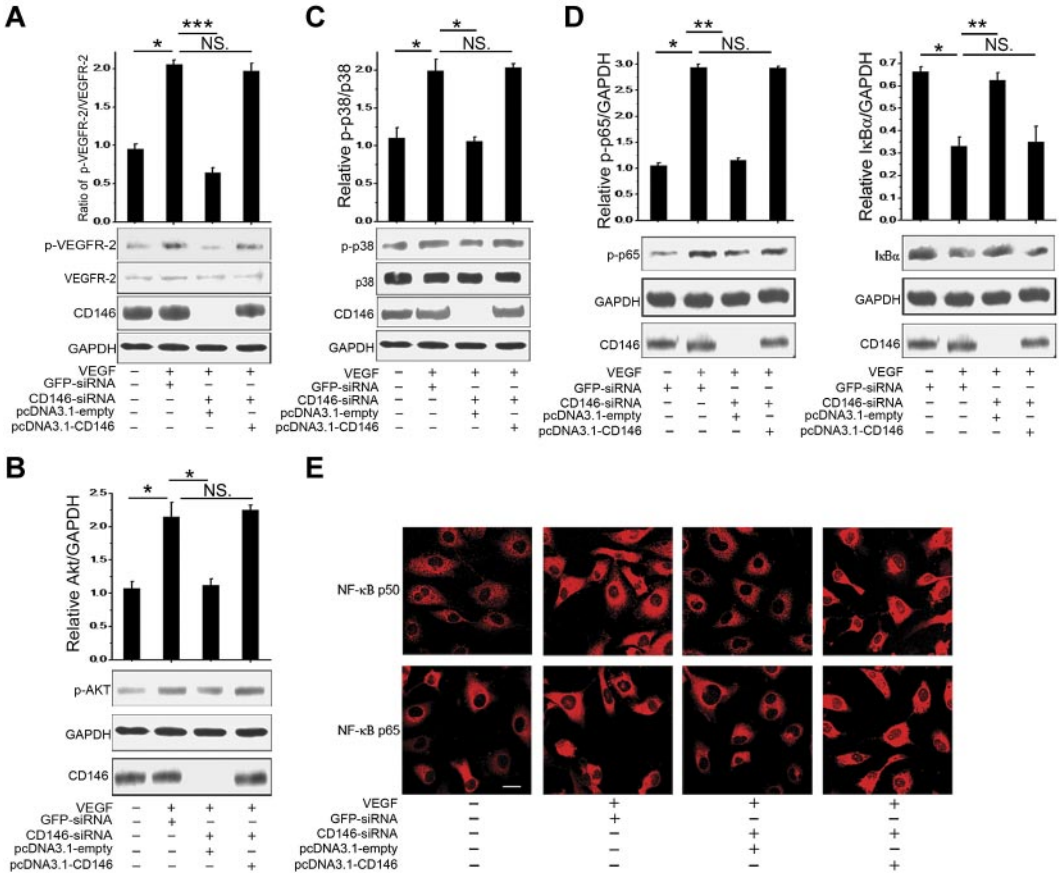

Figure 3. CD146 is required for VEGF-mediated signal transduction. (A) Phosphorylation of VEGFR-2 induced by VEGF was determined after HUVECs were cotransfected with CD146-siRNA and pcDNA3.1-CD146. The quantification of the relative p-VEGFR-2/VEGFR-2 index is shown. At least 3 independent assays were performed. (B) AKT activation induced by VEGF was measured after HUVECs were cotransfected with CD146-siRNA and pcDNA3.1-CD146. (C) P38 activation. (D) NF-κB activation induced by VEGF after rescuing CD146 expression. Western blots were quantified by measuring the band density, which was then normalized to GAPDH. Bar graphs (means ± SEM) present normalized values from at least 3 independent experiments. (E) Immunofluorescence showing the role of CD146 in NF-κB nuclear translocation. NF-κB was detected using specific anti-p65 (red) and anti-p50 Abs (red, scale bar indicates 20 μm). $*P < .05$; $**P < .01$; $***P < .001$. NS indicates not significant.

promotion of cell migration. The conserved positively charged amino acid cluster KKGK motif is responsible for the interaction of CD146 and ERM in this process.[25] It has been shown that some coreceptors, such as CD44, interact with ERM proteins and the cytoskeleton to promote signaling efficiently. CD44v6, VEGFR-2/c-Met, ERMs, and the cytoskeleton form a signalosome.[25,28] To evaluate whether this mechanism is also essential for VEGFR-2 signaling, we transfected HUVECs with a CD146 construct lacking the KKGK motif (CD146-△KKGK) or a moesin construct lacking the actin-binding domain (MSN-△ABD). As shown in Figure 4A-B, we found that either CD146-△KKGK or MSN-△ABD disturbed VEGF-induced VEGFR-2 downstream signaling without affecting VEGFR-2 phosphorylation. In addition, HUVECs transfected with CD146-△KKGK or MSN-△ABD showed a loss of migration capability (Figure 4C-D). These data suggest that the interaction of CD146 and ERM is essential for VEGF-induced signal transduction and cell migration.

CD146 is required in cell migration and tube formation induced by VEGF

To investigate the function of CD146 in the VEGF-promoted angiogenesis process, we performed endothelial cell migration and tube-formation assays in the presence of AA98 and AA1. First, we tested the role of CD146 in VEGF-induced endothelial cell migration. As shown in Figure 5A, VEGF-induced motility of HUVECs was suppressed strongly by AA98, but not by AA1.

In addition, VEGF-stimulated cell migration was significantly impaired after CD146 knock-down in HUVECs and was rescued after transfection with a CD146-expressing construct. Quantification of the number of migrated cells revealed a 1.5-fold increase in VEGF-stimulated HUVEC migration that was abrogated by CD146-siRNA treatment (Figure 5C).

Next, we examined the function of CD146 on in vitro angiogenesis induced by VEGF. A tube-formation assay was performed by growing endothelial cells in Matrigel with either anti-CD146 Ab AA98 or AA1. Results showed that VEGF promoted endothelial tubular morphogenesis and accelerated tube formation. However, in the presence of AA98, the length of vessels decreased by 50% compared with that in the presence of AA1 (Figure 5B). This VEGF-promoted tube formation was also found to be suppressed markedly when CD146 was knocked down in HUVECs by transfecting with CD146-siRNA. Tubular morphogenesis could be rescued by restoring CD146 levels (Figure 5D).

We also found that the CD146-mediated tube formation is specifically dependent on VEGF, because when TNFα was used as a stimulator, neither CD146 knockdown nor anti-CD146 AA98 affected the angiogenic process (supplemental Figure 4). This may

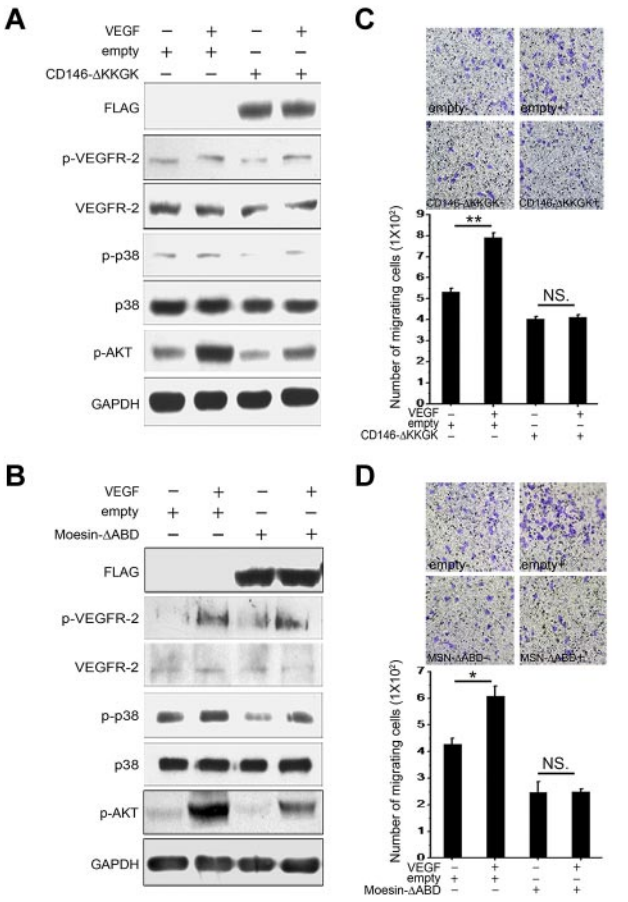

Figure 4. VEGFR-2 signaling is dependent on CD146 binding to Moesin. (A) A CD146-△KKGK was transfected transiently into HUVECs and activation of VEGFR-2 induced by VEGF and signaling to AKT and p38 was determined. (B) Moesin-△ABD was transfected transiently into HUVECs and activation of VEGFR-2 on induction with VEGF and signaling to AKT or p38 were determined. (C-D) The migrating capability of HUVECs induced by VEGF was determined after transfection with CD146-△KKGK or Moesin-△ABD. Cell migration was determined using a Transwell system as described in "Cell migration assay." Data were collected from 3 wells. Representative images of migrated cells are also shown. $*P < .05$; $**P < .01$. NS indicates not significant.

also help to explain the more profound effect of AA98 on angiogenesis in vitro than in vivo.

VEGF-induced angiogenesis is impaired in CD146$^{EC\text{-}KO}$ mice

To explore the potential role of CD146 in VEGF-mediated angiogenesis in vivo, we used a Matrigel plug model in which Matrigel mixed with VEGF is injected subcutaneously into age- and sex-matched CD146$^{EC\text{-}KO}$ and wild-type mice. In this system, endothelial cells migrate into the Matrigel and form a capillary network. One week after implantation, the numbers of blood vessels were counted by immunofluorescence using the blood vessel marker CD31. Our results showed that the microvascular density of the Matrigel plugs in CD146$^{EC\text{-}KO}$ mice decreased to 47% compared with that of the wild-type mice and no large vascular tubes were seen (Figure 6), indicating that the VEGF-induced angiogenic response is dependent on CD146 in vivo.

AA98 and bevacizumab cumulatively inhibit human pancreatic carcinoma growth

It has been well documented that tumor growth is dependent on angiogenesis, and both AA98 and bevacizumab have been reported previously to inhibit tumor angiogenesis.[12,29,30] Our finding that CD146 acts as a coreceptor for VEGFR-2 prompted us to investigate whether AA98 and bevacizumab could produce an additive effect on inhibiting tumor growth. We developed a tumor model using the human pancreatic carcinoma cell line SW1990, which express neither CD146 nor VEGFR-2 (supplemental Figure 5). Therefore, neither AA98 nor bevacizumab could target the actual tumor cells and therefore any reduction in tumor growth would be the result of an antiangiogenic effect. Ab treatment was started when tumors reached a diameter of 5-6 mm. Our results showed that the growth of the human pancreatic carcinoma cells was markedly suppressed by treatment with AA98, bevacizumab, and AA98 + bevacizumab. A significant reduction in the tumor volume and weight was seen in the AA98- or bevacizumab-treated groups compared with the control groups treated with mIgG, hIgG, and AA1, suggesting a

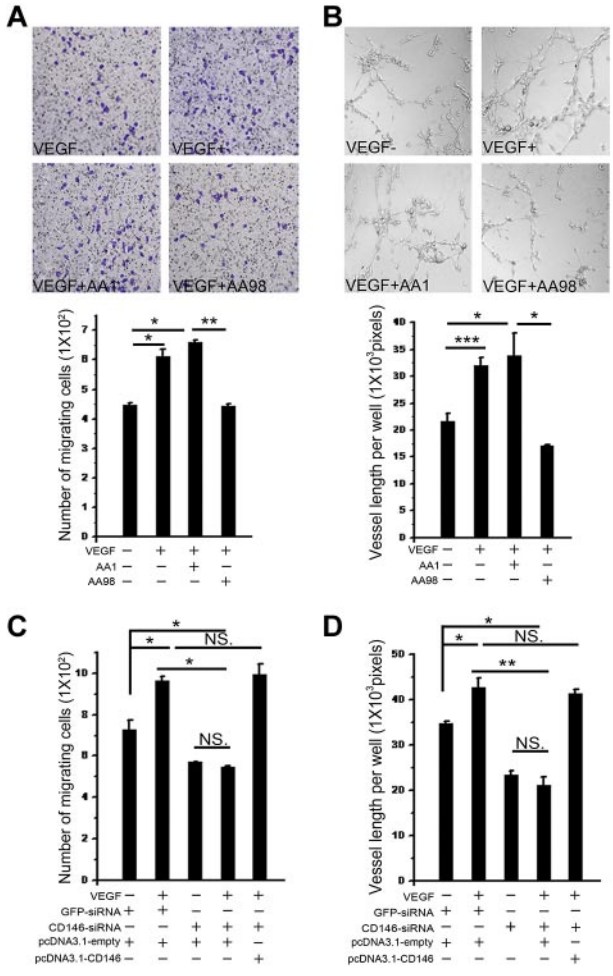

Figure 5. CD146 is required in VEGF-induced cell migration and tube formation. (A) Cell migration was determined using a Transwell system. HUVECs were induced by VEGF in the presence of anti-CD146 mAbs AA98 or AA1. The migrating cells were counted. Data were collected from 3 wells. Representative images of migrated cells are also shown. (B) VEGF-induced tube formation was quantified in the presence of anti-CD146 mAb AA98 or AA1 by counting the total vessel length per field. Data were collected from 3 wells. (C) Cells cotransfected with CD146-siRNA and pcDNA3.1-CD146 were subjected to cell-migration assays and the number of cells migrating through the filters was recorded. The number of cells per optic field is presented as the mean ± SEM of at least 3 independent assays. (D) Cells cotransfected with CD146-siRNA and pcDNA3.1-CD146 were subjected to tube-formation assays. Results presented are total tube lengths from 3 independent tests (means ± SEM). $*P < .05$; $**P < .01$; $***P < .001$. NS indicates not significant.

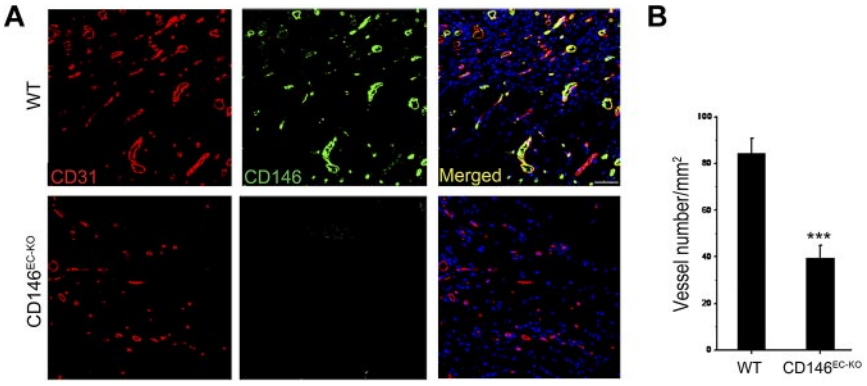

Figure 6. VEGF-induced vascularization is impaired in CD146^{EC-KO} mice. (A) Immunofluorescence showing the vascularization induced by VEGF in the Matrigel explanted in wild-type (WT) and CD146^{EC-KO} mice. Staining of blood vessels was performed with a CD31 Ab (red); green indicates CD146 (rat anti-CD146, ME-9F1) staining. Nuclei were stained with DAPI (blue). Ten mice were included in each group. Bar represents 50 μm. (B) The graph represents average vessel number in 5 random fields of each section. ***$P < .001$.

role for CD146 and VEGF in pancreatic carcinoma growth. It is interesting that the combinatorial treatment with AA98 and bevacizumab had a significant inhibitory effect on the growth of the pancreatic tumor (70%) that was more efficient than AA98 (46%) or bevacizumab (48%) alone (Figure 7A-C; $P < .001$, AA98 + bevacizumab vs AA98; $P < .001$, AA98 + bevacizumab vs bevacizumab), suggesting that the 2 agents act, at least in part, on different pathways.

In immunohistochemical analysis of the treated tumors, we observed a significant reduction of microvessel density in both the AA98- and the bevacizumab-treated groups. However, in the AA98 + bevacizumab combination-treated group, the vessel numbers were approximately 40% and 30% less than that of AA98 or bevacizumab treatment alone, respectively (Figure 7D). We also found this additive effect of AA98 and bevacizumab on another tumor model: human melanoma xenografted mice with A375 cells (supplemental Figure 6).

These data suggest that the combination of AA98 with bevacizumab to target tumor angiogenesis could eventually be used in a clinical setting.

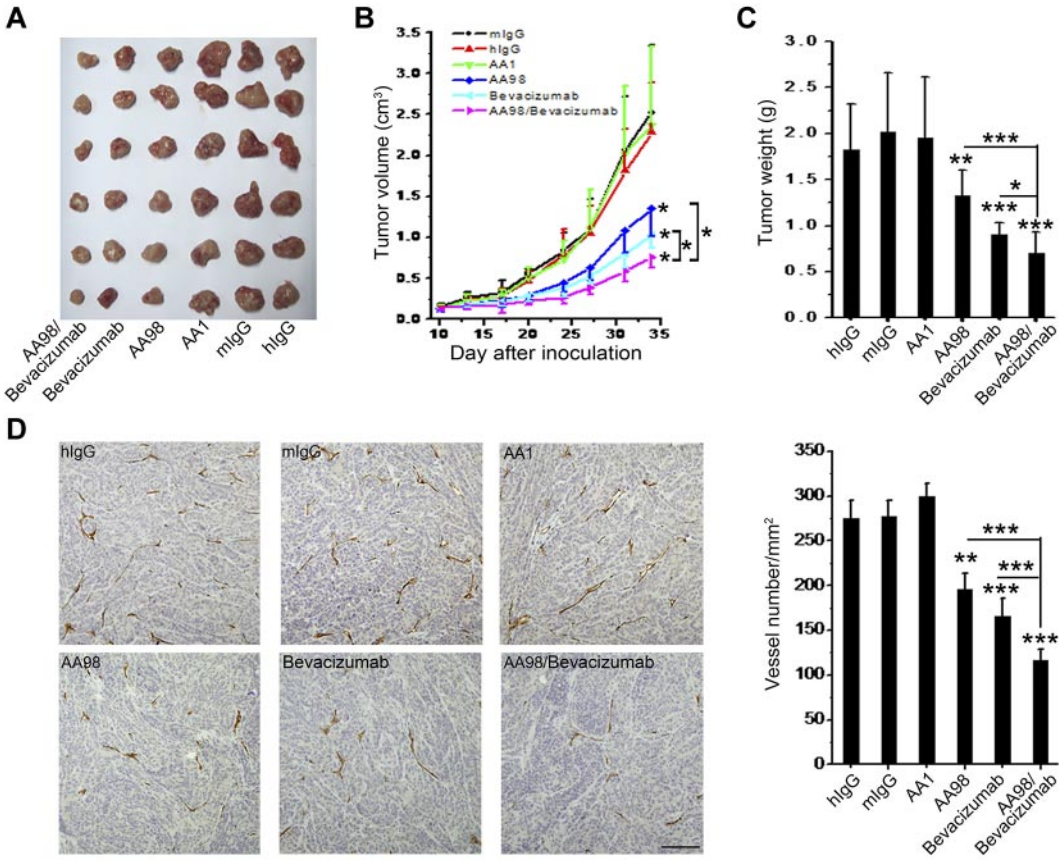

Figure 7. The combination of anti-CD146 AA98 and anti-VEGF bevacizumab has cumulative antitumor effects on human pancreatic carcinoma growth and angiogenesis in vivo. (A) Representation of human pancreatic carcinoma in xenografted mice. (B) Mean tumor volumes at specific time points after injection of human pancreatic carcinoma cells SW1990 (n = 10). (C) When tumor size reached approximately 3 cm^3, mice were killed and tumors were excised and weighed. Tumor weight was evaluated and is shown in the graphs. (D) Microvascular density of tumors. Sections from human pancreatic carcinoma were stained with anti-CD31 Ab (scale bar indicates 100 μm). Statistical significance was calculated with the unpaired Student *t* test. *$P < .05$; **$P < .01$; ***$P < .001$.

Discussion

There is increasing evidence supporting a role for CD146 in angiogenesis.[12,15] We hypothesized that a possible link between CD146 and VEGFR-2 existed because both are endothelial markers and involved in Akt and p38 MAPK downstream signaling to promote endothelial cell migration and angiogenesis. However, there has been no direct evidence demonstrating the relationship between CD146 and VEGFR-2. In the present study, we show for the first time that CD146 interacts directly with VEGFR-2 in endothelial cells and functions as a coreceptor for VEGFR-2 to enhance VEGF-induced signal transduction and angiogenesis. Several lines of evidence support the role of CD146 as a coreceptor for VEGFR-2. First, the interaction of CD146 and VEGFR-2 was detected not only on endothelial cells that endogenously express both molecules, but also in VEGFR-2–transfected HEK293T cells and between the 2 soluble molecules. The structural basis for this interaction is located in the extracellular domain around amino acid 452 of CD146, because the CD146/C452A mutant and anti-CD146 (AA98) targeting C452-C499 could block this interaction. However, a different anti-CD146 (AA1) targeting amino acids 50-54 did not affect the CD146–VEGFR-2 interaction. Second, CD146 enhanced VEGF-induced VEGFR-2 phosphorylation and downstream signaling, which leads to cell migration and blood vessel formation. Furthermore, VEGF-induced AKT/p38 MAPK/NF-κB signals could be abolished by the CD146-specific Ab AA98 and CD146 siRNA. In addition, our in vivo angiogenesis assay showed that vascularization is significantly impaired in $CD146^{EC\text{-}KO}$ mice. Lastly, the combination of anti-CD146 AA98 and anti-VEGF bevacizumab showed an additive function in the treatment of human pancreatic carcinoma and melanoma in xenografted mice.

Although several VEGFR-2 coreceptors,[31-35] including Neuropilin-1,[36] Neuropilin-2,[37] and CD44v6,[28] have been reported to play a role in VEGFR-2 signaling and angiogenesis, we found that, unlike Neuropilin-1 and Neuropilin-2, which have interactions with VEGFR-2 that are dependent on VEGF treatment and mainly involved in the VEGFR-2-Erk pathway (which eventually results in cell proliferation), the interaction of CD146 with VEGFR-2 is independent of VEGF treatment (data not shown) and is involved in the VEGF-mediated p38 MAPK and AKT signaling pathways (which culminate in cell migration). These observations suggest that the different VEGFR-2 coreceptors may trigger different downstream signals, resulting in different cell functions. Therefore, it is of particular interest to elucidate the function of these coreceptors (eg, CD146, CD44v6, and Neuropilin-2) in VEGF-mediated angiogenesis.

There also exists a common mechanism for VEGFR-2 coreceptor signaling. Both the cytoplasmic tail of CD146 and CD44 recruit ERM proteins and cytoskeleton for VEGF-induced signal transduction, suggesting that a scaffold is necessary for linking the intracellular signaling molecules together at the docking site of VEGFR-2. In addition, as is the case for PDGFRs, which have no known coreceptor, ERMs are needed for signal transduction.[38] Binding of ERM proteins to the cytoskeleton may thus be a common mechanism essential for signal transduction.

Based on all of these observations, we conclude that the regulation of CD146 as a VEGFR-2 coreceptor in the VEGF signaling pathway and angiogenesis acts in 2 ways: (1) the extracellular domain of CD146 interacts directly with VEGFR-2 and forms a complex with VEGFR-2 and VEGF, which is a crucial step for VEGFR-2 activation; and (2) the cytoplasmic tail of CD146 recruits ERMs and cytoskeleton, assembling the signalsome required for signal transduction from VEGFR-2 to AKT and p38 MAPKs.

In the SW1990 tumor model, we made use of bevacizumab, an anti-VEGF Ab, as a combination partner for AA98. We believe that bevacizumab mediated its antitumor effect primarily through the blocking of VEGF–VEGFR-2 signaling rather than VEGFR-1, although VEGF-A can bind both. This is because the 2 VEGF receptors differ in their binding affinities to VEGF-A and their function in angiogenesis. The binding of VEGF-A to VEGFR-2 on endothelial cells results in the phosphorylation of VEGFR-2 and angiogenesis. However, the interaction of VEGF-A with VEGFR-1 acts as a negative regulator of angiogenesis because of the weaker phosphorylation of VEGFR-1, although the binding affinity of VEGF-A to VEGFR-1 is stronger than VEGFR-2.[39,40] In addition, our new data showing that CD146 does not interact with VEGFR-1 on endothelial cells (supplemental Figure 7) suggests that the effect of bevacizumab on tumor angiogenesis occurs primarily through VEGFR-2 rather than VEGFR-1, even though VEGF-A binds both VEGFR-2 and VEGFR-1.

Interestingly, AA98 and bevacizumab combination therapy shad an additive effect on tumor angiogenesis in the SW1990 tumor model, which is in agreement with another study showing synergistic, proangiogenic effects between soluble CD146 and VEGF.[41] Therefore, the synergistic effect between the combined Abs is because of the incomplete overlapping signaling of CD146 and VEGFR-2. In previous studies, we and others have found that CD146 can also function independently of VEGFR-2.[13,21,41] In addition, VEGF can signal, at least in part, independently of CD146. For example, the ERK pathway cannot be inhibited by anti-CD146 AA98 nor CD146-siRNA and other VEGF receptors such as VEGFR-1 can transduce VEGF signals. (supplemental Figure 7). This may help to explain why anti-CD146 (AA98) in our combined-therapy model did not inhibit angiogenesis completely.

AA98's targeting of CD146 in combination with bevacizumab could be exploited as a valid regimen in clinical therapy. Our finding provides a novel approach to inhibit tumor angiogenesis. Bevacizumab, a humanized mAb targeting VEGF-A, is one of the most popular antiangiogenesis drugs and precedents exist for its use in combination with other agents in tumor therapy, including in colorectal cancer,[42] nonsquamous-cell lung carcinoma, metastatic renal cell carcinoma, and glioblastoma multiforme.[43] However, the challenge of bevacizumab is its limited clinical application because of its effectiveness only on certain types of cancer.[44] For example, bevacizumab is not very efficient for pancreatic cancer.[45] Therefore, the dual targeting of CD146 and VEGF could prove to be more efficient for the treatment of pancreatic cancer and melanoma. This is the first report of the effectiveness of bevacizumab combinatorial therapy with a second Ab in the inhibition of tumors. In addition, bevacizumab was found to be effective only in metastatic colorectal cancer but not on stage II and III tumors,[46] suggesting that angiogenesis in the primary and metastatic tumor involve different mechanisms that require different treatments. CD146 has been implicated in the tumor progression of several cancers, including colorectal cancer,[47] epithelial ovarian cancer,[48] and breast cancer.[18] Therefore, bevacizumab in combination with anti-CD146 mAb AA98 may be a more effective treatment for metastatic tumors. However, this needs further investigation. In

conclusion, the results of the present study provide evidence of a novel VEGFR-2 coreceptor and a promising strategy for combinatory antiangiogenic therapy.

Acknowledgments

The authors thank Prof Lena Claesson-Welsh for providing the human VEGFR-2 gene-containing pcDNA3.1/myc-His(+)B-VEGFR-2 plasmids and Dr Irene Gramaglia for editing the manuscript.

This work was supported in part by grants from the National Basic Research Program of China (973 program; 2012CB934003, 2011CB915502, 2009CB521704, and 2011CB933503); the National Important Science and Technology Specific projects (2012ZX10002-009, 2008ZX10004-005, and 2009ZX09102-247); the National Natural Science Foundation of China (91029732 and 20872173); and the Knowledge Innovation Program of the Chinese Academy of Sciences (KSCX2-YW-M15).

Authorship

Contribution: T.J. designed and performed the experiments, analyzed the data, and wrote the manuscript; J.Z. and Y.L. assisted with the design of the experiments and analyzed the data and images; H.D., Y.L., and Q.Z. assisted with the animal experiments; K.F. constructed the C452A mutation of the CD146 gene; H.Y. assisted with the experiments relating to signaling pathways; D.L. performed the cell-culture experiments; Z.Y. assisted with experiments relating to signaling pathways and reviewed the manuscript; J.H. assisted with the immunohistochemical analyses; J.F. and D.Y. assisted with data analysis; and X.Y. designed the project and the experiments, analyzed the data, and reviewed the manuscript.

Conflict-of-interest disclosure: The authors declare no competing financial interests.

Correspondence: Xiyun Yan, Institute of Biophysics, Chinese Academy of Sciences, 15 Datun Road, Beijing 100101, China; e-mail: yanxy@ibp.ac.cn.

References

1. Carmeliet P, Jain RK. Molecular mechanisms and clinical applications of angiogenesis. *Nature.* 2011;473(7347):298-307.
2. Grothey A, Galanis E. Targeting angiogenesis: progress with anti-VEGF treatment with large molecules. *Nat Rev Clin Oncol.* 2009;6(9):507-518.
3. Tugues S, Koch S, Gualandi L, et al. Vascular endothelial growth factors and receptors: anti-angiogenic therapy in the treatment of cancer. *Mol Aspects Med.* 2011;32(2):88-111.
4. Kaipainen A, Korhonen J, Mustonen T, et al. Expression of the fms-like tyrosine kinase 4 gene becomes restricted to lymphatic endothelium during development. *Proc Natl Acad Sci U S A.* 1995;92(8):3566-3570.
5. Potente M, Gerhardt H, Carmeliet P. Basic and therapeutic aspects of angiogenesis. *Cell.* 2011; 146(6):873-887.
6. Hurwitz H, Fehrenbacher L, Novotny W, et al. Bevacizumab plus irinotecan, fluorouracil, and leucovorin for metastatic colorectal cancer. *N Engl J Med.* 2004;350(23):2335-2342.
7. Sandler A, Gray R, Perry MC, et al. Paclitaxel-carboplatin alone or with bevacizumab for non-small-cell lung cancer. *N Engl J Med.* 2006; 355(24):2542-2550.
8. Yang JC, Haworth,L, Sherry RM, et al. A randomized trial of bevacizumab, an anti-vascular endothelial growth factor antibody, for metastatic renal cancer. *N Engl J Med.* 2003;349(5):427-434.
9. Miller K, Wang M, Gralow J, et al. Paclitaxel plus bevacizumab versus paclitaxel alone for metastatic breast cancer. *N Engl J Med.* 2007;357(26): 2666-2676.
10. Van Cutsem E, Lambrechts D, Prenen H, et al. Lessons from the adjuvant bevacizumab trial on colon cancer: what next? *J Clin Oncol.* 2011; 29(1):1-4.
11. Lehmann JM, Riethmuller G, Johnson JP. MUC18, a marker of tumor progression in human melanoma, shows sequence similarity to the neural cell adhesion molecules of the immunoglobulin superfamily. *Proc Natl Acad Sci U S A.* 1989; 86(24):9891-9895.
12. Yan X, Lin Y, Yang D, et al. A novel anti-CD146 monoclonal antibody, AA98, inhibits angiogenesis and tumor growth. *Blood.* 2003;102(1):184-191.
13. Kang Y, Wang F, Feng J, et al. Knockdown of CD146 reduces the migration and proliferation of human endothelial cells. *Cell Res.* 2006;16(3): 313-318.
14. So JH, Hong SK, Kim HT, et al. Gicerin/Cd146 is involved in zebrafish cardiovascular development and tumor angiogenesis. *Genes Cells.* 2010; 15(11):1099-1110.
15. Bu P, Gao L, Zhuang J, et al. Anti-CD146 monoclonal antibody AA98 inhibits angiogenesis via suppression of nuclear factor-kappaB activation. *Mol Cancer Ther.* 2006;5(11):2872-2878.
16. Liu Q, Yan X, Li Y, et al. Pre-eclampsia is associated with the failure of melanoma cell adhesion molecule (MCAM/CD146) expression by intermediate trophoblast. *Lab Invest.* 2004;84(2):221-228.
17. Liu Q, Zhang B, Zhao X, et al. Blockade of adhesion molecule CD146 causes pregnancy failure in mice. *J Cell Physiol.* 2008;215(3):621-626.
18. Zeng Q, Li W, Lu D, et al. CD146, an epithelial-mesenchymal transition inducer, is associated with triple-negative breast cancer. *Proc Natl Acad Sci U S A.* 2012;109(4):1127-1132.
19. Ouhtit A, Gaur RL, Abd Elmageed ZY, et al. Towards understanding the mode of action of the multifaceted cell adhesion receptor CD146. *Biochim Biophys Acta.* 2009;1795(2):130-136.
20. Bu P, Zhuang J, Feng J, et al. Visualization of CD146 dimerization and its regulation in living cells. *Biochim Biophys Acta.* 2007;1773(4):513-520.
21. Zheng C, Qiu Y, Zeng Q, et al. Endothelial CD146 is required for in vitro tumor-induced angiogenesis: the role of a disulfide bond in signaling and dimerization. *Int J Biochem Cell Biol.* 2009; 41(11):2163-2172.
22. Anfosso F, Bardin N, Frances V, et al. Activation of human endothelial cells via S-endo-1 antigen (CD146) stimulates the tyrosine phosphorylation of focal adhesion kinase p125(FAK). *J Biol Chem.* 1998;273(41):26852-26856.
23. Anfosso F, Bardin N, Vivier E, et al. Outside-in signaling pathway linked to CD146 engagement in human endothelial cells. *J Biol Chem.* 2001; 276(2):1564-1569.
24. Zhang Y, Zheng C, Zhang J, et al. Generation and characterization of a panel of monoclonal antibodies against distinct epitopes of human CD146. *Hybridoma (Larchmt).* 2008;27(5):345-352.
25. Luo Y, Zheng C, Zhang J, et al. Recognition of CD146 as an ERM-binding protein offers novel mechanisms for melanoma cell migration. *Oncogene.* 2012;31(3):306-321.
26. Nagata D, Mogi M, Walsh K. AMP-activated protein kinase (AMPK) signaling in endothelial cells is essential for angiogenesis in response to hypoxic stress. *J Biol Chem.* 2003;278(33):31000-31006.
27. Redmond EM, Cullen JP, Cahill PA, et al. Endothelial cells inhibit flow-induced smooth muscle cell migration: role of plasminogen activator inhibitor-1. *Circulation.* 2001;103(4):597-603.
28. Tremmel M, Matzke A, Albrecht I, et al. A CD44v6 peptide reveals a role of CD44 in VEGFR-2 signaling and angiogenesis. *Blood.* 2009;114(25): 5236-5244.
29. Yancopoulos, G.D. Clinical application of therapies targeting VEGF. *Cell.* 2010;143(1):13-16.
30. Bevacizumab. Anti-VEGF monoclonal antibody, avastin, rhumab-VEGF. *Drugs R D.* 2002;3(1):28-30.
31. Orian-Rousseau V, Chen L, Sleeman JP, et al. CD44 is required for two consecutive steps in HGF/c-Met signaling. *Genes Dev.* 2002;16(23): 3074-3086.
32. Pályi-Krekk Z, Barok M, Kovacs T, et al. EGFR and ErbB2 are functionally coupled to CD44 and regulate shedding, internalization and motogenic effect of CD44. *Cancer Lett.* 2008;263(2):231-242.
33. Meran S, Luo DD, Simpson R, et al. Hyaluronan facilitates transforming growth factor-beta1-dependent proliferation via CD44 and epidermal growth factor receptor interaction. *J Biol Chem.* 2011;286(20):17618-17630.
34. Olaku V, Matzke A, Mitchell C, et al. c-Met recruits ICAM-1 as a coreceptor to compensate for the loss of CD44 in Cd44 null mice. *Mol Biol Cell.* 2011;22(15):2777-2786.
35. Francavilla C, Loeffler S, Piccini D, et al. Neural cell adhesion molecule regulates the cellular response to fibroblast growth factor. *J Cell Sci.* 2007;120(Pt 24):4388-4394.
36. Whitaker GB, Limberg BJ, Rosenbaum JS. Vascular endothelial growth factor receptor-2 and neuropilin-1 form a receptor complex that is responsible for the differential signaling potency of VEGF(165) and VEGF(121). *J Biol Chem.* 2001; 276(27):25520-25531.
37. Favier B, Alam A, Barron P, et al. Neuropilin-2 interacts with VEGFR-2 and VEGFR-3 and promotes human endothelial cell survival and migration. *Blood.* 2006;108(4):1243-1250.
38. Voltz JW, Brush M, Sikes S, et al. Phosphorylation of PDZ1 domain attenuates NHERF-1 binding to cellular targets. *J Biol Chem.* 2007;282(46): 33879-33887.

39. Sawano A, Iwai S, Sakurai Y, et al. Flt-1, vascular endothelial growth factor receptor 1, is a novel cell surface marker for the lineage of monocyte-macrophages in humans. *Blood.* 2001;97(3):785-791.
40. Waltenberger J, Claesson-Welsh L, Siegbah A, et al. Different signal transduction properties of KDR and Flt1, two receptors for vascular endothelial growth factor. *J Biol Chem.* 1994;269(43):26988-26995.
41. Harhouri K, Kebir A, Guillet B, et al. Soluble CD146 displays angiogenic properties and promotes neovascularization in experimental hindlimb ischemia. *Blood.* 2010;115(18):3843-3851.
42. Escudier B, Pluzanska A, Koralewski P, et al. Bevacizumab plus interferon alfa-2a for treatment of metastatic renal cell carcinoma: a randomised, double-blind phase III trial. *Lancet.* 2007;370(9605):2103-2111.
43. Friedman HS, Prados MD, Wen PY, et al. Bevacizumab alone and in combination with irinotecan in recurrent glioblastoma. *J Clin Oncol.* 2009;27(28):4733-4740.
44. Van Meter ME, Kim ES. Bevacizumab: current updates in treatment. *Curr Opin Oncol.* 2010;22(6):586-591.
45. Van Cutsem E, Vervenne WL, Bennouna J, et al. Phase III trial of bevacizumab in combination with gemcitabine and erlotinib in patients with metastatic pancreatic cancer. *J Clin Oncol.* 2009;27(13):2231-2237.
46. Allegra CJ, Yothers G, O'Connell MJ, et al. Phase III trial assessing bevacizumab in stages II and III carcinoma of the colon: results of NSABP protocol C-08. *J Clin Oncol.* 2011;29(1):11-16.
47. Adachi K, Hattori M, Kato H, et al. Involvement of gicerin, a cell adhesion molecule, in the portal metastasis of rat colorectal adenocarcinoma cells. *Oncol Rep.* 2010;24(6):1427-1431.
48. Aldovini D, Demichelis F, Doglioni C, et al. M-CAM expression as marker of poor prognosis in epithelial ovarian cancer. *Int J Cancer.* 2006;119(8):1920-1926.

2012 120: 2330-2339
doi:10.1182/blood-2012-01-406108 originally published online June 20, 2012

CD146 is a coreceptor for VEGFR-2 in tumor angiogenesis

Tianxia Jiang, Jie Zhuang, Hongxia Duan, Yongting Luo, Qiqun Zeng, Kelong Fan, Huiwen Yan, Di Lu, Zhongde Ye, Junfeng Hao, Jing Feng, Dongling Yang and Xiyun Yan

Blood (print ISSN 0006-4971, online ISSN 1528-0020), is published weekly by the American Society of Hematology, 2021 L St, NW, Suite 900, Washington DC 20036.